

Article

Biodiesel Production Potential from Littered Edible Oil Fraction Using Directly Synthesized S-TiO₂/MCM-41 Catalyst in Esterification Process via Non-Catalytic Subcritical Hydrolysis

Md Sufi Ullah Siddik Bhuyan ¹, Abul Hasnat Md Ashraf Alam ¹, Younghwan Chu ² and Yong Chan Seo ^{1,*}

¹ Department of Environmental Engineering, Sangji University, Usan-dong, 83 Sangjidae-gil, Wonju-si, Gangwon-do 26339, Korea; siddikdcc@gmail.com (M.S.U.S.B.); ahasnat08@gmail.com (A.H.M.A.A.)

² CNS Scientific, 2710-1 Bugwonro, Wonju-si, Gangwon-do 26316, Korea; twozero2@gmail.com

* Correspondence: ycseo@sangji.ac.kr; Tel.: +82-33-730-7525; Fax: +82-33-730-0444

Academic Editor: Thomas E. Amidon

Received: 22 June 2017; Accepted: 23 August 2017; Published: 29 August 2017

Abstract: Due to uncontrolled consumption of fossil fuel it is necessary to use alternative resources as renewable energy. Among all the available liquid fuels biodiesel has drawn attention for producing less emissions and having less aromatic contents than diesel and because it can also be obtained from inferior grade feedstocks. Since the various uses of fats and oils have increased, a significant amount of waste animal fat and used edible oil is generated every year. In this work, we produced biodiesel from littered edible oil fraction (LEOF) via hydrolysis followed by catalytic esterification. Nearly 90% free fatty acids (FFA) content was achieved at 275 °C, after 45 min during hydrolysis and linoleic acid (C18:2) was observed to be the highest component. Compared to refined soybean oil (SBO) the reaction rate was accelerated by the auto-catalytic behavior of free fatty acids (FFA) in littered edible oil fraction (LEOF). For catalytic esterification, S-TiO₂/MCM-41 catalyst was directly synthesized and characterized by using XRD, SEM, NH₃-TPD and Brunauer Emmett Teller (B.E.T). The parameters such as; SO₄²⁻ content, TiO₂ loading and calcination temperature were varied to get optimum free fatty acids (FFA) conversion. Fatty acid methyl ester (FAME) conversion was 99.29% using 1% S-TiO₂/MCM-41 catalyst at 240 °C whereas 86.18% was observed with 3.5% catalyst at 180 °C with 20 min. Thus, using S-TiO₂/MCM-41 catalyst in esterification via hydrolysis would be a better option for treating low quality feedstocks.

Keywords: sustainable; littered edible oil fraction; sub-critical; hydrolysis; auto-catalytic; esterification

1. Introduction

With the increasing global trend in natural resources consumption, the supply of fossil fuels is going to start to diminish. As a result, the reserves are going down and with the rising demand, the price is increasing dramatically. To meet this challenge, it is critical today for scientists and researchers to focus on identifying cost-effective, renewable and environmentally friendly different options to produce bio-fuel. Among all the available liquid fuels compatible with diesel fuel, biodiesel has drawn attention as it is nontoxic, bio-degradable, sulfur free, has a low flash point, produces less emissions and has lower aromatic contents [1]. First generation biodiesel, produced from edible oil feedstocks, represents a more sustainable source of renewable energy, but in the long run it will not be socially and economically viable as it requires a significant share of the available edible oil crops for fuel production. To overcome these challenges, there is a growing demand for non-edible/unproductive sources of feedstocks, called 2nd generation biodiesel, to produce renewable fuel all over the world [2]. Therefore,

lands can be devoted to growing non-edible feedstocks, and provide a more sustainable energy source in the near future. For the last decades, due to flexibility and reliability concerns, researchers have been trying to identify biodiesel sources, and numerous studies have been performed to identify the suitable energy efficient crops for the quality biodiesel production. Good progress has already been achieved in this area with the introduction of more than 350 oil-bearing crops for the production of biodiesel [3,4]. Moreover, the quality and suitability of biodiesel produced from renewable feedstocks as a replacement for petroleum fuel are still uncertain [2]. Recently, macadamia oil has been found a potential candidate for biodiesel production and it can be used in diesel engines where up to 20% blends with diesel fuel can be used without any engine optimization [5]. Therefore, the selection of feedstocks, whether edible or non-edible feedstocks, for biodiesel production, mostly depends on technical and economic viability so that they can be used extensively on a fully commercial scale, and unfortunately, the evolution of research to focus on these issues is not developing firmly. Thus, the uses of both edible and non-edible feedstock sources still has limitations, as it can impose a burden on food security and require extra agricultural land area, finally increasing the production cost of biodiesel. Compared to those feedstocks, littered edible oil fraction (LEOF), a non-arable waste, which is less expensive than vegetable oil, is a promising alternative feedstock that could be a good replacement for edible/non-edible oil bearing crops [6]. It can reduce production costs by almost 45%, with additional pretreatment cost [7]. Biodiesel production from littered edible oil fraction can save about 21% fossil energy in comparison to the use of crude oil, and an energy saving of 96% compared to fossil diesel production. Each kilogram of littered edible oil fraction can be converted into 0.92 kg–0.97 kg of biodiesel [8]. Moreover, regarding environmental performance concerns, around 27% CO₂ emission savings occurs annually during energy production from vegetable oil/biodiesel [9].

Recently, with rapid changes in food consumption habits and lifestyle, and the availability of many processed products, the industrial and non-food uses of fats and oils have increased. As a result, a significant amount of waste animal fat and used cooking oil are generated every year, and many regions of the world are suffering from difficulties in its disposal. Usually, it is just drained into nearby sewers, creating an ecological and environmental imbalance, as sewage effluent treatment costs are increased. Meanwhile, some developed countries are setting good policies and rules to ban littered oil discharge whereas the Asian world is generally unaware of its proper management. This problem can be mitigated and managed efficiently by utilizing littered edible oil fraction as a fuel source [10].

Biodiesel can be produced by transesterification using homogeneous alkali, acid, and enzymatic catalysts. Two distinct factors: less reaction time and low cost are involved in alkali and acid catalyzed transesterification compared to the enzyme catalyst process [11,12]. To get high yields and better quality biodiesel, alkali catalyst treatment is the most appealing process, but it requires high-grade feedstocks as it is very sensitive to foreign bodies in the edible/non-edible oils, such as water and free acids [13]. A two-step transesterification process (the first step being an esterification process under acid catalysis followed by alkali-catalyzed transesterification) has been studied to maintain a high content of acids and improve the biodiesel quality, but this requires longer reaction times and the low catalyst recovery disfavor this process [14]. The homogeneous Lewis acid catalysts used to solve this problem persist in the two-step process. It also requires too high temperatures and gives relatively low yields. Alternatively, supercritical methanol (SCM) transesterification has been used for a variety of feedstocks without employing any catalyst. It can handle a high content of impurities and produces a high yield of biodiesel [15]. However, it requires a well-engineered process to provide the rigorous temperature and pressure conditions that can productively recover the spent energy [16], which in turn involves very high capital cost and is difficult to use on an industrial scale. A different route, SCM esterification of fatty acids via hydrolysis, was also studied to optimize SCM transesterification. Kusdiana and Saka [17] successfully employed this process, firstly to convert the feedstock oil into fatty acids (FAs) and then converting the FAs into fatty acid methyl esters under supercritical conditions. Littered edible oil fraction (LEOF), a substitute feedstock was also used to optimize SCM transesterification [17]. One downside is that the supercritical methanol (SCM)

process requires special alloys for reactors such as Inconel or Hastelloy which can sustain a high pressure-temperature environment, which negatively affects the production cost and also may lead to degradation of the products. Inconel or Hastelloy are mainly Ni-based superalloy materials having properties such as high temperature strength, excellent corrosion resistance, good ductility, oxidation resistance, microstructural stability, mechanical formability and castability [18].

It is still a challenging task to identify an efficient process that can use a low-quality feedstock and abilities to avoid denaturation of the product with less effort. As biodiesel is susceptible to denaturation at elevated temperatures when using littered edible oil fraction, catalytic treatment at lower temperatures would be a better option. Moreover, this would also allow the use of common stainless steel instead of special alloys for reactors. Since the presence of water and free fatty acids in the low-quality feedstock is unavoidable, it is more desirable to hydrolyze triglycerides to fatty acids, and then esterified these catalytically into fatty acid methyl esters (FAMES).

In consideration of environmental and economic reasons, many researchers have made great efforts to replace conventional acid catalysts with the newer solid super acid catalysts. This has resulted in a great advancement for biodiesel production for both free fatty acid (FFA) esterification and triglyceride transesterification [19]. The reactions are more tolerant to the presence of water and free fatty acids (FFAs) [20]. The use of solid superacids has advantages such as a high concentration of catalytic sites, no corrosion of the reactor, ease of handling, less cost and they are easy to recover and reuse over the long-term as compared to homogeneous liquid acids and solid base catalysts [21,22]. Among all these prepared solid acid catalysts, TiO₂-based catalysts have attracted worldwide attention for their varied applications in many organic reactions [23,24]. They have been used as supports and prime catalysts. MgO/TiO₂ mixed oxide catalysts prepared by the sol-gel method were successfully used for biodiesel production, but their catalytic activity decreased slowly during reuse [25]. The transesterification reaction of vegetable oils is also performed using superacid sulfated nanosized TiO₂ catalysts. These displayed good catalytic activity, but the biodiesel yield was not significant [26]. A new type of solid superacid catalyst, (SO₄²⁻/ZrO₂-TiO₂) loaded with lanthanum, was also proved to be an effective catalyst for both transesterification and esterification using 60% acid-containing feedstocks. The yield was found to be around 90% and the catalyst could be used as many as five times, but it requires a longer reaction time, the catalyst cost is high and it is difficult to filter the tiny particles, which limits its application on an industrial scale [27]. To overcome those problems, a sustainable and low-cost SO₄²⁻/TiO₂-SiO₂ solid acid catalyst having large particles was also examined for biodiesel production using low-value feedstocks. Unfortunately, the relatively small surface area and low reaction rate may limit its usefulness in catalytic activities [28,29]. To increase the surface area and pore volume the thermally resistant mesoporous silica (MCM-41) support has been introduced to prepare a new type of S-TiO₂/MCM-41 composites, an inexpensive good superacid solid catalyst for esterification and transesterification processes. It has received good attention due to its large surface area, easy regeneration and reutilization features and for being able to maintain its acidity after high-temperature calcination (773 K to 873 K) [30]. After calcination, the MCM-41 and transition metal compounds were found to agglomerate, and the metals were dispersed onto as well as inside the mesoporous structure. S-TiO₂/MCM-41 still retained up to 80 wt % of the metal loading on or inside the MCM-41 mesoporous structure after high-temperature calcination [29]. Hence, S-TiO₂/MCM-41 solid super acid catalyst may exhibit excellent catalytic activity during the esterification process.

In this work, we have focused on managing the littered edible oil fraction efficiently by producing biodiesel. We investigate the hydrolysis of LEOF followed by catalytic esterification to produce biodiesel. There are two parts of this study. In first step, hydrolysis will be performed using both littered edible oil fraction (LEOF) and refined soybean oil (SBO) under non-catalytic subcritical conditions and in 2nd step we performed a catalytic esterification under both subcritical and supercritical conditions. To perform the esterification, we also synthesized S-TiO₂/MCM-41 composites by the direct impregnation method as solid superacid catalyst. Although some organic reactions have done previously by S-TiO₂ with synthesized MCM-41, directly impregnated S-TiO₂/MCM-41 composites has

never been investigated for the esterification of hydrolyzed littered edible oil fraction. The successful development of such a process would greatly increase the prospects of using a low-quality feedstock for economical biodiesel production. The directly synthesized S-TiO₂ supported on MCM-41 is expected to have the ability to alleviate the severe reaction conditions of the supercritical methanol (SCM) method to produce biodiesel from littered edible oil fraction.

2. Materials and Methods

2.1. Materials

Two independent samples of raw littered edible oil fraction (LEOF) and refined soybean oil (SBO) were collected from a restaurant and a grocery shop located in Sangji University, Wonju-si, and Gangwon-do, South Korea on different days and stored under ambient conditions until the pretreated samples were used for fatty acid production.

Deionized water was obtained a Milli-Q reverse osmosis purification system (Fisher Scientific, Bedford, MA, USA). Anhydrous sodium sulfate 98.5% was purchased from Samchun Pure Chemical Co., Ltd. (Seoul, Korea). Reagent grade chemicals: 99.9% anhydrous ethyl alcohol, > 99.0% diethyl ether, > 95.0% sulfuric acid (H₂SO₄), and > 85.0% potassium hydroxide (KOH) were purchased from Daejung Chemical & Metals Co., Ltd. (Busan, Korea). All chemicals are of analytical grade and used without further purification. 99% Palmitic acid, 99% stearic acid, 99% oleic acid, 99% linoleic acid and 99% linolenic acid standards and 99% heptadecanoic acid used as internal standard (I.S.) were obtained from Sigma-Aldrich. Co. (St. Louis, MO, USA). Methyl alcohol and $\geq 96\%$ *n*-hexene, used as a solvent for GC analysis, were also purchased Daejung Chemical & Metals Co., Ltd. Reference FAME Mix RM-3 was obtained from Supelco (Bellefonte, PA, USA), and internal standard methyl heptadecanoate (C17:0 $\geq 96\%$) was purchased from Sigma-Aldrich Co. An analytical sample was prepared by mixing 1 mL of diluted sample with 1 mL I.S in a vial and then injecting using the autosampler (model-8200 CX, Varian, Milpitas, CA, USA) is a gas chromatography system. For catalyst synthesis CTAB, Pluronic (P123, PEO₂₀PPO₇₀PEO₂₀) and TiO₂ (21 nm) > 99.5% were obtained from Sigma-Aldrich Co. To produce the Ti(OH)₄ precursor, titanium sulfate (> 24%) purchased from Fisher Scientific (Loughborough, UK) was used. Tetraethyl orthosilicate (C₈H₂₀O₄Si $\geq 98\%$) was purchased from ACROS Organics Co. (Morris Plains, NJ, USA).

2.2. Methods

2.2.1. Preparation of S-TiO₂/MCM-41

To prepare the S-TiO₂/MCM-41 composite titania sulfate was directly impregnated onto the as-synthesized silicate composite instead of impregnating them onto a calcined MCM-41 material with the desired amount of titanium sulfate solution using a literature method [29]. First, distilled water was applied to dissolve cetyltrimethyl ammonium bromide (CTAB) in a 2M NaOH solution and titanium sulfate solution. Once fully dissolved, the silica source, tetraethoxysilane (TEOS), was added dropwise to the mixture with vigorous stirring at room temperature. The mole composition of the gel mixture was CTAB:TEOS:NaOH:H₂O:80% Ti(SO₄)₂; 1.0:3.75:1.64:434 and the TiO₂ content was taken to be 80%. The pH of the mixture was maintained at 10.2 with 30% ammonia. After heating at 100 °C for two days, the product was filtered, washed, dried at 80 °C overnight, and then calcined at 550 °C for 7h @ 1.83 °C/min. To optimize reaction condition with maximum yield, here we varied TiO₂ loading, H₂SO₄ concentration, and calcination temperatures.

2.2.2. Reaction Process

A 500 mL 316 stainless steel batch reactor vessel (Ø88, 110 L, Hanwoul Eng. Co., Ltd., Model HR-8302, Gyeonggi-do, Korea) with a glass liner was used for both the hydrolysis and esterification reactions. Typically, 100 g of substrate was charged into the reaction cell for each run.

Temperature (225 °C–275 °C), substrate mole ratio (1:50–1:75; littered/soybean cooking oil: DI water) and time (15–60 min) were varied to study the effect of reaction conditions during non-catalytic hydrolysis. At the end of each run, the cell was depressurized to atmospheric pressure through the sampling valve and quenching in a cold water bath.

In the experiments, the collected water phase came out milky white, indicating an emulsion containing free fatty acids had formed. Glycerol is mainly responsible for making this milky white water phase during non-catalytic hydrolysis. Hence, approximately 1 g–2 g of salt (Na_2SO_4) was added to the hydrolyzed product to remove water and salt-out the fatty acids. After hydrolysis, the reaction mixture was extracted with diethyl ether. Then the products were separated into an oil phase and a water phase in a phase separator. The oil phase (upper portion) consists mainly of FFA, while the water phase (lower portion) contains the glycerol. The ether was then evaporated to leave oil consisting of the hydrolyzed fatty acids and any unreacted triglycerides. Samples were immediately transferred to a weighing flask and kept in a light protected laboratory case at 4 °C prior to analysis. This extract was then subjected to a volumetric titration method to determine the degree of hydrolysis. For confirmation of individual composition, GC analysis was also performed. A gravimetrically measured one μL aliquot of oil sample (FFA) was injected in splitless mode into a gas chromatography (GC) system using a Varian 3400 Gas chromatography unit equipped with a flame ionization detector. For fatty acid (FA) separation, a Stabilwax-DA GC column (Cat. No. 11025, 30 m \times 0.53 mm \times 0.25 μm , Restek, Bellefonte, PA, USA) was used. The GC oven initial temperature was 40 °C and it was increased to 160 °C at a ramp rate of 6 °C/min, followed by a second temperature ramp of 15 °C/min to 250 °C then held for 10 min. Injector and detector temperatures were both 280 °C. Nitrogen was used as the carrier gas at a constant flow rate 30 mL/min. The total flow of gas was maintained at 350 mL/min. External standards ranging from carbon chain lengths of 16–18 were used to construct calibration curves for quantitatively determining the FA concentration of samples. Retention times for this set of standards ranged from 26 min to 38 min. The littered edible oil fraction and refined soybean oil are composed almost exclusively of triglycerides (TGs). The distribution of the FA chain length of hydrolyzed littered edible oil fraction was found to be 16% palmitic acid, 4% stearic acid, 27% oleic acid, 51% linoleic acid, and 2% linolenic acid. For refined soybean oil we observed 15% palmitic acid, 4% stearic acid, 23% oleic acid, 40% linoleic acid, and 18% linolenic acid. The average molecular weight of fatty acid (FA) in the littered edible oil fraction was calculated to be around 280 g/mol.

The degree of hydrolysis was determined by titration of the oil phase samples with 0.1 N potassium hydroxide (KOH). For each sample, 5 g of the oil phase was dissolved in 25 mL ethanol: diethyl ether (1:2 *v/v*). The amount of 0.1 N KOH required to neutralize the acid was noted. A blank titration was done as control samples. Phenolphthalein was used as an indicator.

For methyl esterification of free fatty acids (FFA), a similar experimental procedure as described above was employed. To recover S-TiO₂/MCM-41 solid superacid from the end product, we used vacuum filtration with Whatman-55 filter paper for further use. The reaction time was set for 20 min and the temperature was maintained within 180 °C to 280 °C. During esterification, catalytic and non-catalytic conditions were also studied. The effectiveness of sulfated titanium oxide supported MCM-41 catalyst and with varying TiO₂ loading, SO₄²⁻ content and calcination temperatures were examined during the esterification process to optimize the reaction conditions. The products were analyzed by gas chromatography (Varian, 3400 CX) with a DB-5 capillary column (30 m \times 0.25 mm \times 0.25 μm film thickness) and a flame ionization detector (FID). The weights of methyl esters produced were determined by comparing the peaks detected in the samples to pure standards. All experiments were carried out in triplicate to obtain average values for the biodiesel conversion.

3. Results and Discussion

3.1. Hydrolysis of Triglycerides in Subcritical Water

3.1.1. Effect of Reaction Temperature

Hydrolysis reactions were carried out at various temperatures ranging from 225 °C to 275 °C with varying molar ratios of oil/water 1:50 and 1:75 (1:1 *v/v* and 1:1.25 *v/v*) for both littered edible oil fraction and refined soybean oil. The triglyceride conversion at a high temperature of 275 °C was almost same for both LEOF and SBO (Table 1).

Table 1. Hydrolysis of littered edible oil fraction (LEOF) and soybean oil (SBO) at various temperatures and reaction times.

Reaction Conditions		LEOF		SBO	
		X _{TG} (%) (Avg)		X _{TG} (%) (Avg)	
t (min)	T (°C)	1:50 o/w	1:75 o/w	1:50 o/w	1:75 o/w
15	225	5.19	4.85	0.86	1.34
15	250	18.32	25.95	3.74	4.59
15	275	36.71	54.91	27.92	49.95
30	225	7.78	7.57	2.37	1.70
30	250	45.35	31.02	26.68	24.50
30	275	82.53	74.26	83.79	77.44
45	225	25.33	17.40	17.79	16.73
45	250	74.07	61.77	64.69	65.28
45	275	84.50	80.36	86.41	83.88
60	225	28.15	21.89	27.86	21.51
60	250	78.60	82.57	80.49	72.47
60	275	92.55	91.79	89.54	91.85

t: time; T: temperature; X_{TG}: conversion of triglycerides; o/w: oil to water mole ratio.

Figure 1 shows that the TG conversion was sharply increased by increasing the reaction temperature and pressure under subcritical conditions, and more FFA content was found in the littered edible oil fraction compared to soybean oil.

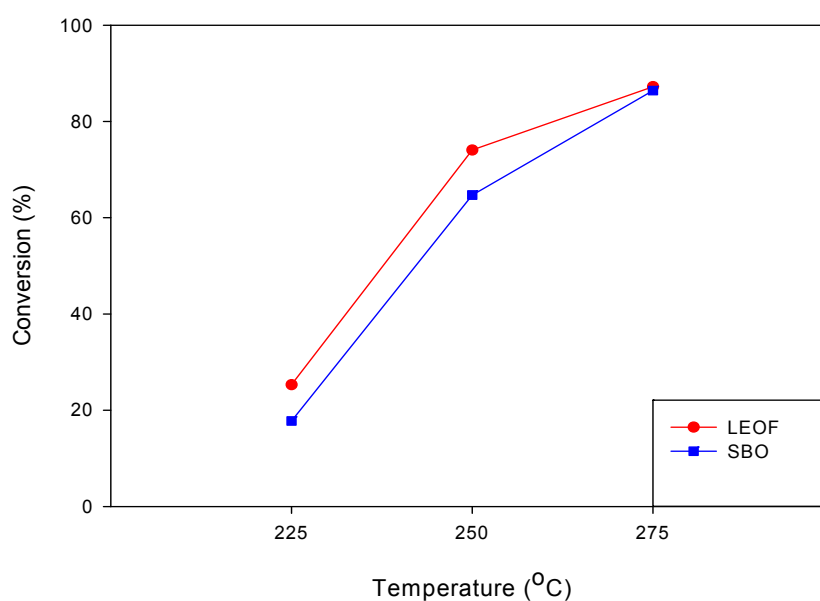


Figure 1. FFA content (%) at various temperatures for 45 min and 1:50 o/w mole ratio.

This was due to the presence of a significant initial amount of FFA in littered edible oil fraction that accelerated the rate of reaction. Minami and Saka revealed that FA plays an important role as an acid catalyst in the hydrolysis reactions of oils/fats in subcritical water [31]. This phenomenon suggests that FA produced by hydrolysis would act as an acid catalyst in subcritical water. The rate becomes higher with the increasing temperature. The mixed littered edible and refined soybean oil are also used to observe the effect of the initial amount of FFA that contributes to enhancing the FFA conversion as shown in Figure 2. Besides that untreated diglycerides and monoglycerides present in frying oil were also hydrolyzed during the hydrolysis step which also might increase the FFA content.

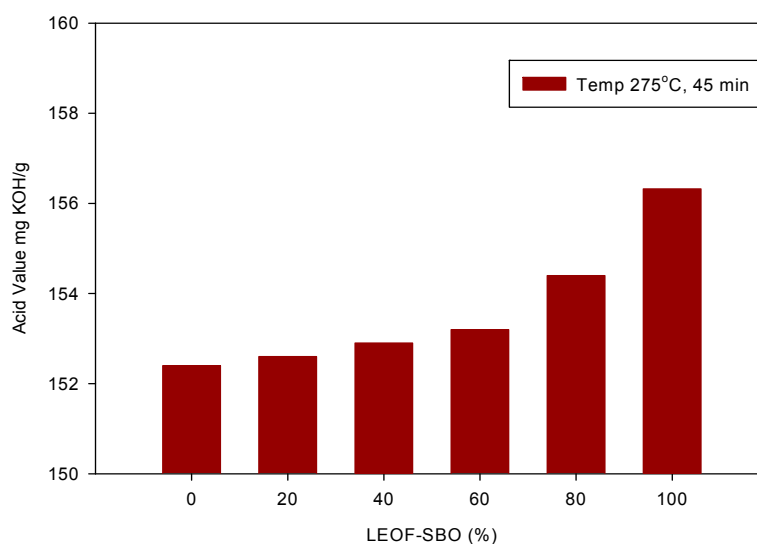


Figure 2. Acid value (mg KOH/g oil) of the hydrolyzed mixed edible oil in subcritical water at 275 °C.

3.1.2. Effect on Reaction Time

Concerning the time course of the yield, FFA yield at 225 °C for the first 15 min was low, around 6% for LEOF and 4% for SBO, respectively. However, it increased with reaction time, and at 225 °C and 60 min, 22% and 10% FFA content was obtained for littered edible oil fraction (LEOF) and refined sobean oil (SBO), respectively. The rate of FFA formation becomes higher with the increasing time as shown in Figure 3.

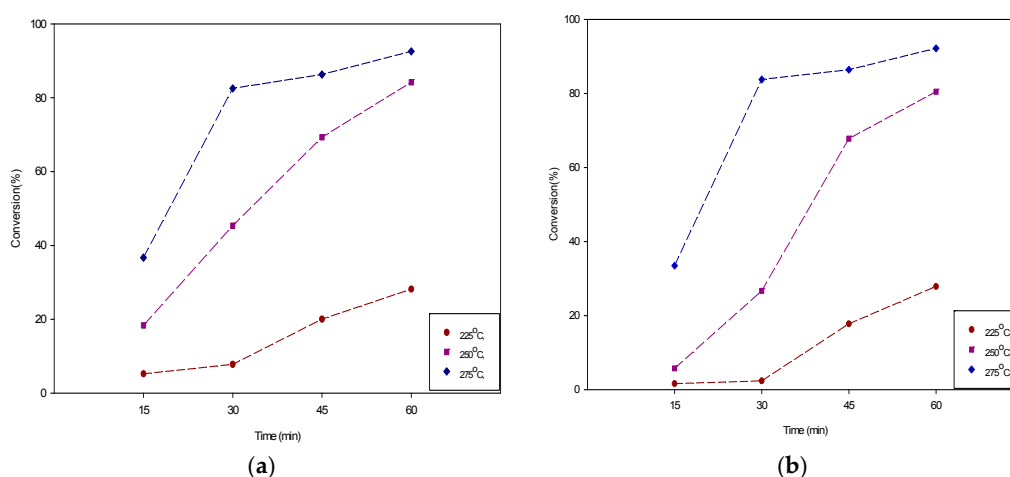


Figure 3. FFA content (%) at various times with temperatures at 225, 250 and 275 °C. (a) Littered edible oil fraction; (b) Soybean Oil.

The highest FFAYield of up to 92% was obtained at 60 min reaction time, 80 bars, 275 °C and 1:50 molar ratio of littered edible oil fraction hydrolysis. The same yield was obtained under the same reaction conditions for soybean oil hydrolysis. The optimum yield was 84.5% observed at 45 min for littered edible oil fraction.

3.2. Catalyst Characterization

For characterization of the catalyst XRD, SEM, NH_3 -TPD and B.E.T. surface area analysis were performed.

3.2.1. X-ray Diffraction

The agglomeration of S-TiO₂ on the MCM-41 support with different TiO₂ loadings following our direct synthesis method was evidenced by XRD (Figure 4). All the samples showed a sharp peak indexed as (100) and smaller peaks indexed as (110), which are typical of 2-D cylindrical (p6 mm) MCM-41 material. The diffraction peak of impregnated S-TiO₂ appeared to have almost the same intensity. The appearance of the main (100) reflection implies the existence of mesopores in all S-TiO₂/MCM-41 samples. Therefore, the finding provided that the mesoporous structure of MCM-41 was not damaged during the solid dispersion process.

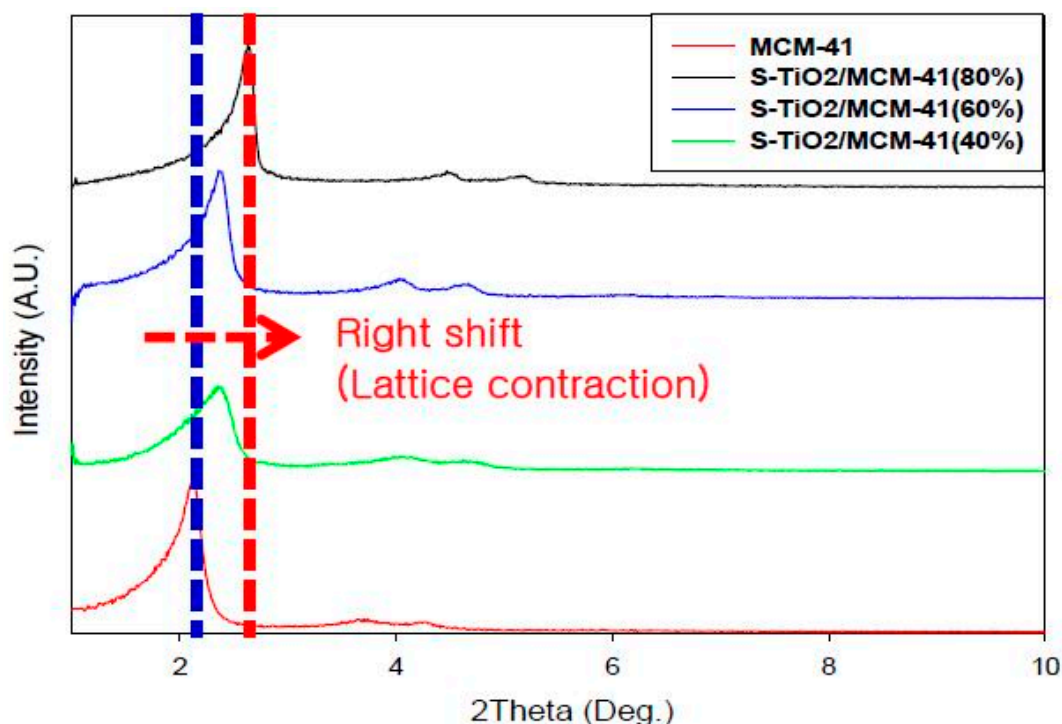


Figure 4. XRD patterns of S-TiO₂/MCM-41 with different TiO₂ contents calcined at 550 °C for 7 h in the air.

3.2.2. SEM Analysis

SEM images of the impregnated mesoporous silicas (TiO₂ loading of 80 wt %) are illustrated in Figure 5. These images demonstrate the surface morphology of the catalysts with different magnifications. A road-like morphology with a clear edge, was observed in mesoporous silica (MCM-41), but it was disappeared gradually with the increasing amount of Ti(SO₄)₂ deposition on the surface of the mesoporous silica. The pores of the impregnated mesoporous silica were cylindrical, analogous to those of pure silica (MCM-41).

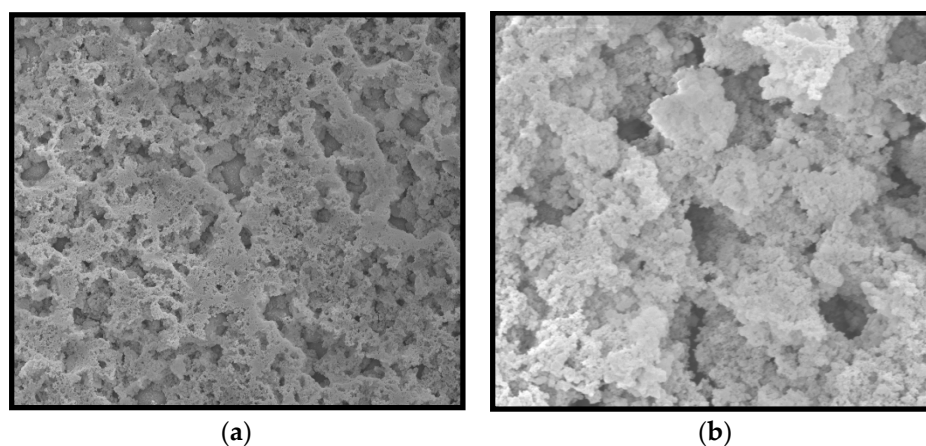


Figure 5. SEM images of S-TiO₂/MCM-41 samples with different magnification; (a) 100 μm; (b) 20 μm.

3.2.3. Physical Properties of the Catalyst

The porosity of the S-TiO₂/MCM-41 samples was evaluated by N₂ adsorption isotherms. Figure 6 shows the N₂ adsorption-desorption isotherms curves for the S-TiO₂/MCM-41 samples. Table 2 shows the physical properties of a series of S-TiO₂/MCM-41 samples calcined at 550 °C.

Table 2. Physical Properties of S-TiO₂/MCM-41 Catalyst.

Loading of TiO ₂	BET Surface Area (m ² /g)	2θ	d ₍₁₀₀₎ (nm)
40% TiO ₂	877.0704	2.35	3.754
60% TiO ₂	863.7089	2.36	3.739
80% TiO ₂	714.9370	2.63	3.355

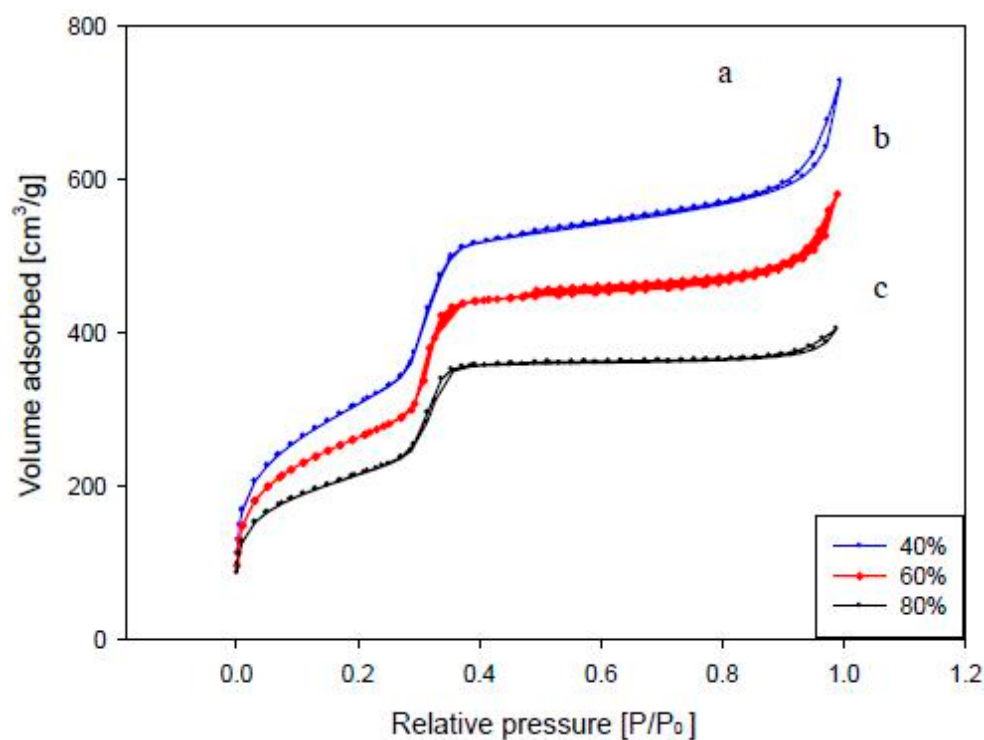


Figure 6. N₂ adsorption-desorption isotherm of various S-TiO₂/MCM-41 samples.

As presented in Figure 6, all the samples showed isotherms of type IV having inflection around $P/P_0 = 0.25\text{--}0.47$, characteristic of the MCM-41 type ordered mesoporous materials. The samples exhibit complementary textural and framework confined mesoporosity, as evidenced by the presence of two separate, well-expressed hysteresis loops. The position of the inflection in the $P/P_0 = 0.25\text{--}0.47$ region depends on the diameter of the mesopores and its sharpness indicates the uniformity of the narrow pore size distribution. It can also be seen in Figure 6 that the point of inflection shifts toward lower relative pressure (P/P_0) with an increase in the TiO_2 content of the S- TiO_2 /MCM-41 samples. This indicates a decrease in the pore size. Moreover, the adsorption curve of S- TiO_2 /MCM-41 samples changed to a curve similar microporous materials, which suggests the incorporation of SO_x and TiO_2 compounds. It can also be noted from Figure 6 that the amount of adsorption of sample 'a' (wt % $\text{TiO}_2 = 40\%$) increased more sharply in the $P/P_0 = 0.35\text{--}0.47$ region than did the amount of adsorption by sample 'c' (wt % $\text{TiO}_2 = 80\%$) in the $P/P_0 = 0.25\text{--}0.4$ region. This suggests that the pore size of sample 'a' is bigger than that of the sample 'c' as the relative pressure P/P_0 of sample 'a' is higher than the sample 'c'.

3.3. Catalytic Activity of S- TiO_2 /MCM-41 in Esterification of FFA in Supercritical and Subcritical Methanol

Methyl esterification of FA is a major reaction to produce FAME in the two-step supercritical methanol process, whereas transesterification of TG is a major one in the conventional alkali and acid-catalyzed methods. This esterification reaction is, therefore, an important step for high-quality biodiesel fuel production. Figure 7 shows typical changes in the yield of FAME when FFAs produced by subcritical hydrolysis were treated in both sub- and supercritical methanol at various conditions. In a similar manner to the hydrolysis reaction, a higher temperature resulted in a faster rate of FAME formation. Also, the yield of FAME tended to increase quickly during the early stage of the reaction, whereas the rate of FAME formation became slow as the reaction proceeded.

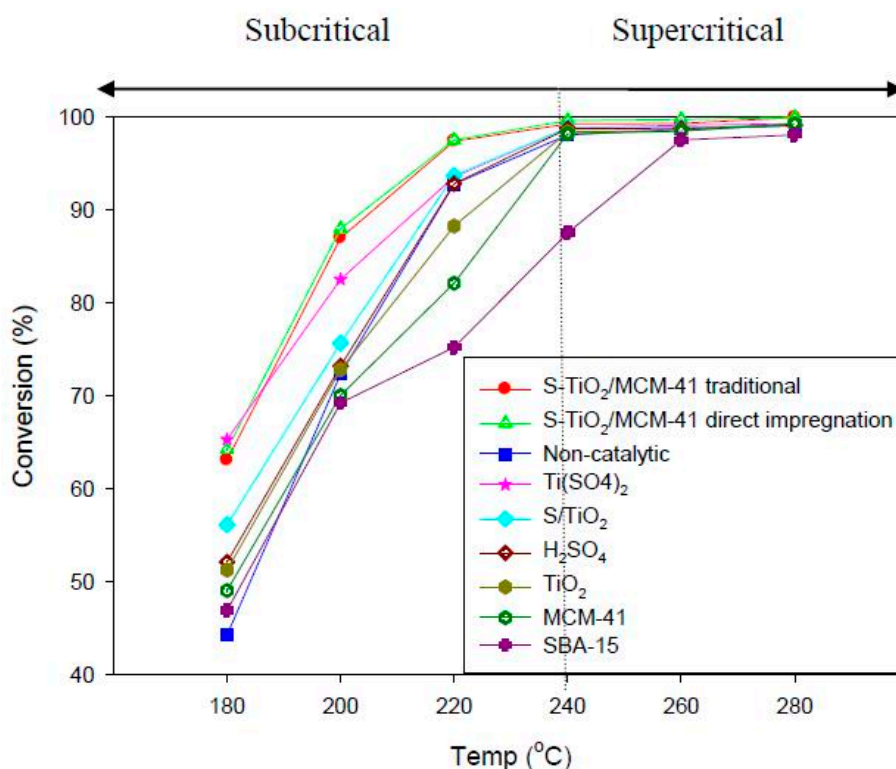


Figure 7. The FAME conversion; temperatures within 180 °C to 280 °C and 20 min.

3.3.1. Effect of TiO₂ Loading

The conversion of FFA as a function of TiO₂ loading as shown in Figure 8. In this study, we varied the TiO₂ loading from 40 wt % to 80 wt % and found the same prismatic structure of catalyst gave an increasing trend of biodiesel production. Even though MCM-41 has little acidity, the composites of TiO₂ and MCM-41 have shown an amazing increase in acidity. This was caused by increasing the specific surface area. The combination of TiO₂ and MCM-41 generated stronger acid sites and more acidity as compared with the separate components. Moreover, modified catalyst with SO₄²⁻ ions had much higher acidity than unmodified catalysts. The catalytic activity of the catalysts depends on the acid sites. TiO₂ content is a key of active sites of S-TiO₂/MCM-41 catalyst. The interaction of TiO₂-MCM-41 complex on the surface with SO₄²⁻ ions produces active sites or acid sites. 80 wt %, the TiO₂ content and specific area is the most favorable, so the conversion of FFA reaches the highest value.

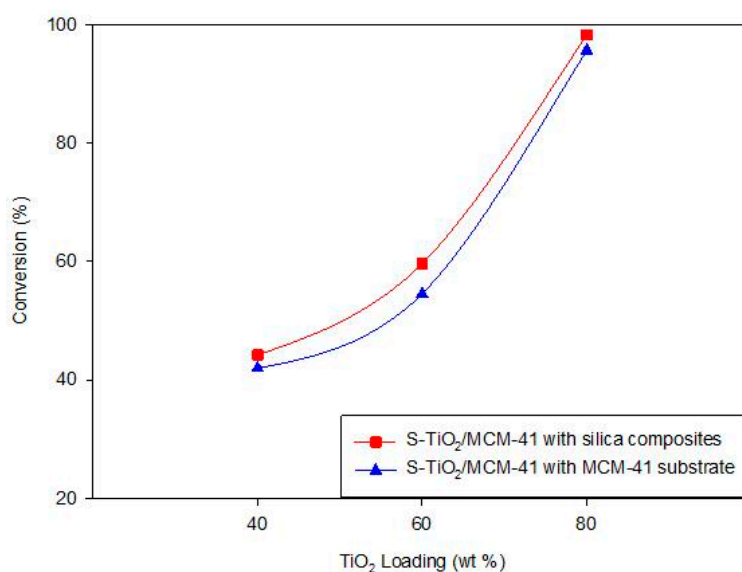


Figure 8. Effect of TiO₂ loading (wt %) of S-TiO₂/MCM-41 sample with silica composites and MCM-41 substrate.

3.3.2. Effect of the Concentration of H₂SO₄ on the of S-TiO₂/MCM-41

We have also studied the effect of concentration of H₂SO₄ during impregnation of the TiO₂-MCM-41 complex and found a positive effect on the activity of the SO₄²⁻/TiO₂-MCM-41 catalyst (Table 3). From Table 3, FFA conversion becomes always low, even when using a concentration of H₂SO₄ higher or lower than 1 M, as there may be a lesser amount of active site interaction between H₂SO₄ and TiO₂. It is confirmed when the H₂SO₄ concentration is higher, it produces more sulfate ions. Through experiments, at the optimum H₂SO₄ concentration of 1 M, the highest conversion rate is achieved.

Table 3. Effect of the different H₂SO₄ concentrations on the conversion of FFA (80% TiO₂ loading) at 220 °C.

H ₂ SO ₄ Concentration (M)	Conversion of FFA (%)
0.25	58.6%
0.50	72.5%
0.75	83.4%
1.0	96.78%
1.25	73.58%

3.3.3. Effect of the Calcination Temperature on the Conversion of FFA

The formation of the active sites of the catalyst mainly depends on the interaction between SO_4^{2-} ions with the TiO_2 -MCM-41 complex at different calcination temperatures, so the calcination temperature of the catalyst is very crucial. It plays an important effect on the activity of the catalysts. It was observed that the conversion of FFA becomes low when the calcination temperature is lower than $500\text{ }^\circ\text{C}$. The conversion rate is quickly decreased again, even after calcination temperature is controlled over $550\text{ }^\circ\text{C}$. It may be due to decomposition of S (sulfur) component on the surface of S- TiO_2 /MCM-41 and the number of active sites decreased. Over $600\text{ }^\circ\text{C}$, much S components are decomposed and the catalyst loses much activity. From Table 4, the optimum calcination temperature is $550\text{ }^\circ\text{C}$ for the S- TiO_2 /MCM-41 composites which produce highest surface area of $714.937\text{ m}^2/\text{g}$.

Table 4. Effect of calcination temperature on the surface area of S- TiO_2 /MCM-41 (80% TiO_2 loading) at $220\text{ }^\circ\text{C}$.

Calcination Temperature ($^\circ\text{C}$)	Specific Surface Area (m^2/g)	Conversion (%)
450	645.527	80%
500	680.355	86%
550	714.937	98%
600	654.326	82%

3.3.4. Stability

One of the important reasons to select solid super acid catalyst is to remove it easily from the final product and its environmental friendliness. Besides that, the reusability properties are another main advantage of using the solid acid catalyst. In this study, we also examined reusability of the catalyst by recycling it. The data of the reusability of the catalysts are presented in Figure 9. S- TiO_2 /MCM-41 has shown more tolerance in nature. Even after the 4th complete reuse run, there is no noticeable change of FAME yield. The experimental results indicate that S- TiO_2 /MCM-41 is a stable catalyst and suitable for long-term use.

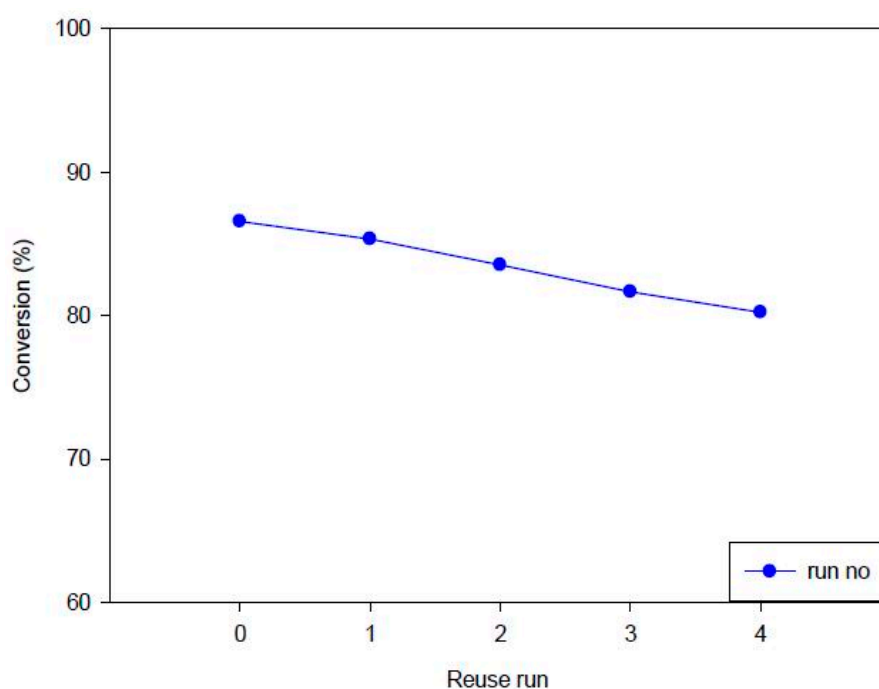


Figure 9. Reusability performance test using several runs of S- TiO_2 /MCM-41 catalyst.

3.3.5. Effect of Different Catalysts for the Yield of Biodiesel

We have investigated catalytic and non-catalytic methyl esterification. We also examined the comparative performance of the catalytic activities of synthesized S-TiO₂/MCM-41 with conventional liquid H₂SO₄, Ti(SO₄)₂ and TiO₂ under sub- and supercritical methanol FFA treatment (shown in Figure 7). Surprisingly, both the parent Ti(SO₄)₂ and the S-TiO₂/MCM-41 catalyst with the maximum TiO₂ content (80 wt %) gave almost similar conversions. The same reaction conditions were also employed for conventional S-TiO₂ with as-synthesized MCM-41 catalyst. It showed lower conversion compared to directly synthesized S-TiO₂/MCM-41 which determined this catalyst was more active than traditional S-TiO₂/MCM-41. In the supercritical range (240 °C–280 °C) a similar trend was observed for all other catalysts, including MCM-41 and SBA-15 silica supports. The elevated temperature was mainly responsible for achieving the higher conversion rather than a catalytic effect. In addition, the high temperature shortened the time required to reach the equilibrium compared to the lower temperature. The reaction reached equilibrium even after the treatment over 240 °C. Meanwhile, the amount of FAME might also increase due to transesterification of unreacted TG, DG and MG with methanol that remained during the hydrolysis stage. It was also verified in another study that if biodiesel (FAME) came only from the conversion of FFAs in SAO (soybean acid oil), the maximum biodiesel yield should not be over 60% under optimized conditions. This indicated that a few glycerides in FFA were transformed into FAME during the transesterification reaction that took place with the esterification reaction [32]. More than 99% FAME conversion found using 1% S-TiO₂/MCM-41 catalyst at 240 °C with 20 min. We also evaluated the surface area of different catalysts and determined the conversion (Table 5).

Table 5. Specific surface area of catalyst sample and effect on the conversion of FFA at 180 °C.

Catalyst	Surface Area (m ² /g)	Conversion (%)
TiO ₂	56.05	51.23
MCM-41	789.0642	49.05
SBA-15	1035.06	46.88
Ti(SO ₄) ₂	-	65.32
H ₂ SO ₄	-	52.12
S-TiO ₂	48.63	56.31
1% S-TiO ₂ /MCM-41 traditional	691.29	63.09
1% S-TiO ₂ /MCM-41 (40% TiO ₂) direct	842.31	44.25
1% S-TiO ₂ /MCM-41 (60% TiO ₂) direct	810.32	59.26
1% S-TiO ₂ /MCM-41 (80% TiO ₂) direct	714.94	64.25
3.5% S-TiO ₂ /MCM-41 (80% TiO ₂) direct	714.94	86.18

Under subcritical conditions (180 °C–240 °C) we have found a remarkable effect using S-TiO₂/MCM-41 catalyst. FAME yield was found about 92% without using catalyst; whereas 98% yield was obtained using 1% S-TiO₂/MCM-41 catalyst at 220 °C and 20 min (Figure 7). Since biodiesel is susceptible to denaturation at a high temperature using littered edible oil fraction, catalytic treatment under low temperature conditions is a better option. Moreover, it allows the use of common stainless steel vessels instead of special alloys for the reactors such as Inconel or Hastelloy. Thus, we varied S-TiO₂/MCM-41 catalyst loading from 1% to 4% and optimum 86.18% yield was observed with 3.5% catalyst at 180 °C with 20 min (shown in Figure 10). Over 3.5% catalyst loading, a sudden drop occurred. It was also observed that individual FAME concentration increases with the increasing temperature and C18:2 was the maximum in all cases (Figure 11). It was also confirmed that acid strength along with high surface area and structural integrity of support contributed a crucial role to enhance the esterification rate. Littered edible oil fraction can be turned into a potential biodiesel product with less effort which may avoid the possibility of denaturation.

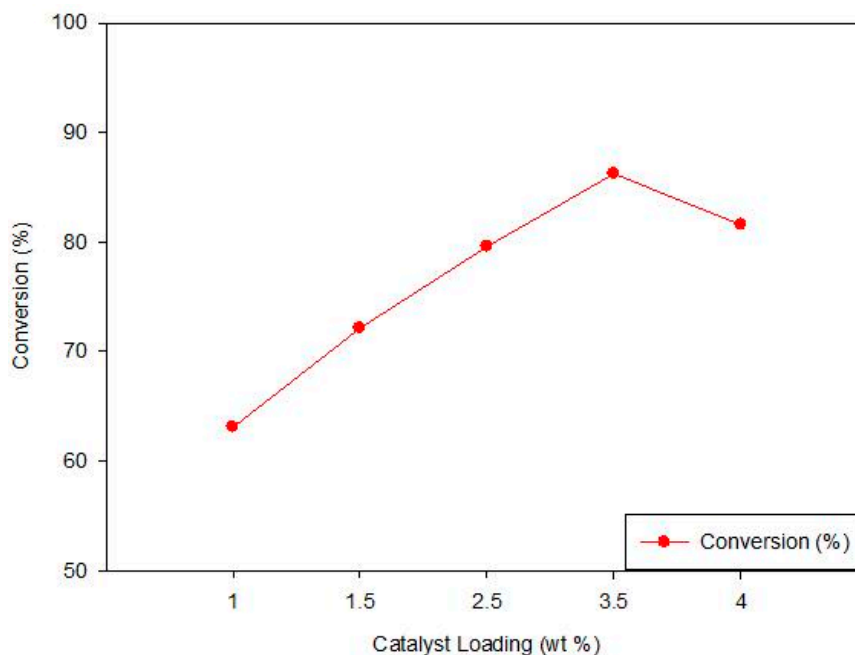


Figure 10. Effect of S-TiO₂/MCM-41 catalyst loading (wt %) at subcritical condition (180 °C, 20 min).

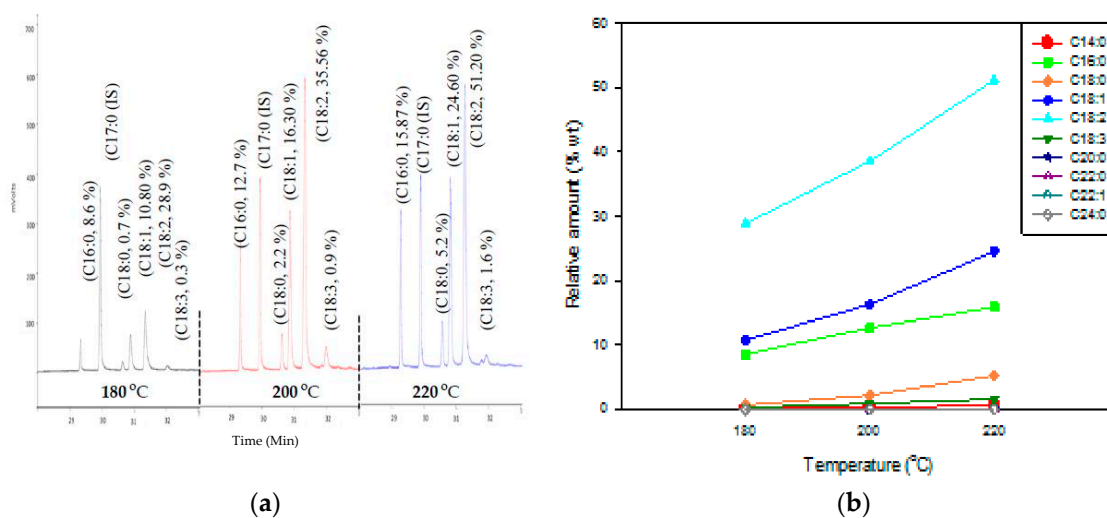


Figure 11. (a) Gas Chromatograph peak of FAME produced from littered edible oil fraction hydrolysis; at 180 °C, 200 °C and 220 °C and 20 min; and (b) Absolute composition (wt %) of individual compound in the FAME.

3.4. Mathematical Calculations

The degree of hydrolysis, X is calculated as below:

$$X\% = \frac{M \times N \times V}{10 \times m}$$

where, X, % = FFA content, %, M = average molecular weight of free fatty acid, in g, N = normality of KOH, V = volume of the KOH solution, in mL, m = weight of the sample, in g.

FAME conversion calculated as below:

Based on the British Standard Specification (British standard method; BS EN14103; 2003), the purity of the FAMES was calculated by using the following formula:

$$\text{Conversion} = [(\Sigma A) - A_{IS}/A_{IS}] \times [(C_{IS} \times V_{IS})/m] \times 100\%$$

where ΣA = the total peak area from the methyl ester in C14:0-C24:1; A_{IS} = internal standard (methyl heptadecanoate) peak area; C_{IS} = concentration of the internal standard solution, in mg/mL; V_{IS} = volume of the internal standard solution used, mL; m = mass of the sample, in mg.

4. Conclusions

Subcritical hydrolysis followed by methyl esterification is an important method for the production of biodiesel from low-valued littered edible oil fraction. Nearly 90% FFA content was achieved by subcritical hydrolysis without employing catalysts at 275 °C, 45 min and linoleic acid (C18:2) was observed to be the highest component. We have also directly synthesized S-TiO₂/MCM-41 catalyst for the esterification step and characterized it by using XRD, SEM, NH₃-TPD and the Brunauer Emmett Teller (B.E.T.) method. The parameters such as SO₄²⁻ content, TiO₂ loading, and calcination temperature were varied to get the optimum conversion. A maximum 80% TiO₂ doped into or outer surface of MCM-41 was achieved. We investigated the comparative catalytic activity performance of directly synthesized S-TiO₂/MCM-41 with conventional liquid H₂SO₄, Ti(SO₄)₂ and TiO₂ under sub- and supercritical methanol treatment of FFA. Surprisingly, both the parent Ti(SO₄)₂ and the S-TiO₂/MCM-41 catalyst with the maximum TiO₂ content (80 wt %) gave almost similar conversion. The same reaction conditions were also employed for conventional S-TiO₂ with as-synthesized MCM-41. It showed lower conversion compared to directly synthesized S-TiO₂/MCM-41 which determined this catalyst was more active than traditional S-TiO₂/MCM-41. A FAME yield of 99.29% (Figure 7) was obtained using 1% S-TiO₂/MCM-41 catalyst at 240 °C and 20 min whereas 86.18% (Figure 10) yield was observed with 3.5% catalyst at 180 °C after 20 min. The increased amount of FAME may be due to transesterification of unreacted TG, DG and MG with methanol remained during the hydrolysis stage. No noticeable change in yield occurred at or above 240 °C with or without catalysis. This indicated that the high temperature mainly facilitated the increase in reaction rate rather than the activity of the catalyst. During subcritical treatment (180 °C–240 °C), however, we have found an excellent effect using directly impregnated S-TiO₂/MCM-41 catalyst by varying the catalyst loading. As a result, the catalytic subcritical methanol esterification process has become a useful and successful method for biodiesel production from littered edible oil fraction and would be able to control the possibility of denaturation. The pore size of MCM-41 was not significantly affected by impregnation of TiO₂ and showed good catalytic activity in the esterification process. The higher FAME yield was obtained relatively at low temperature which could result in high-quality biodiesel compared to the conventional supercritical esterification treatment.

Acknowledgments: This research work was financially supported by Korea Ministry of Environment (MOE) as “Knowledge-based environmental service (Waste to energy recycling) Human Resource Development Project”.

Author Contributions: The contributions of each author are as follows: Md Sufi Ullah Siddik Bhuyan synthesized the catalysts, produced free fatty acids (FFA) and biodiesel (FAME), collected experimental data, analyzed the numerical results, drafted and revised the manuscript according to the reviewer comments; Abul Hasnat Md Ashrafal Alam helped to collect the experimental data and synthesis of catalysts; Younghwan Chu contributed to the experimental design; and Yong Chan Seo checked the revised manuscript.

Conflicts of Interest: The authors declare no conflict of interest.

References

1. Macor, A.; Pavanello, P. Performance and emissions of biodiesel in a boiler for residential heating. *Energy* **2009**, *34*, 2025–2032. [[CrossRef](#)]

2. Jahirul, M.; Brown, R.; Senadeera, W.; O'Hara, I.; Ristovski, Z. The Use of Artificial Neural Networks for Identifying Sustainable Biodiesel Feedstocks. *Energies* **2013**, *6*, 3764–3806. [[CrossRef](#)]
3. Mofijur, M.; Masjuki, H.H.; Kalam, M.A.; Atabani, A.E. Evaluation of biodiesel blending, engine performance and emissions characteristics of *Jatropha curcas* methyl ester: Malaysian perspective. *Energy* **2013**, *55*, 879–887. [[CrossRef](#)]
4. Mofijur, M.; Masjuki, H.H.; Kalam, M.A.; Atabani, A.E.; Fattah, I.M.R.; Mobarak, H.M. Comparative evaluation of performance and emission characteristics of Moringa oleifera and Palm oil based biodiesel in a diesel engine. *Ind. Crops Prod.* **2014**, *53*, 78–84. [[CrossRef](#)]
5. Rahman, M.; Rasul, M.; Hassan, N.; Hyde, J. Prospects of Biodiesel Production from Macadamia Oil as an Alternative Fuel for Diesel Engines. *Energies* **2016**, *9*, 403. [[CrossRef](#)]
6. Canakci, M.; Van Gerpen, J. A pilot plant to produce biodiesel from high free fatty acid feedstocks. *Trans. ASAE* **2003**, *46*, 945–954. [[CrossRef](#)]
7. Escobar, J.C.; Lora, E.S.; Venturini, O.J.; Yáñez, E.E.; Castillo, E.F.; Almazan, O. Biofuels: Environment, technology and food security. *Renew. Sustain. Energy Rev.* **2009**, *13*, 1275–1287. [[CrossRef](#)]
8. Corral Bobadilla, M.; Lostado Lorza, R.; Escribano García, R.; Somovilla Gómez, F.; Vergara González, E. An Improvement in Biodiesel Production from Waste Cooking Oil by Applying Thought Multi-Response Surface Methodology Using Desirability Functions. *Energies* **2017**, *10*, 130. [[CrossRef](#)]
9. De Santoli, L.; Mancini, F.; Nastasi, B.; Piergrossi, V. Building integrated bioenergy production (BIBP): Economic sustainability analysis of Bari airport CHP (combined heat and power) upgrade fueled with bioenergy from short chain. *Renew. Energy* **2015**, *81*, 499–508. [[CrossRef](#)]
10. Kulkarni, M.G.; Dalai, A.K. Waste cooking oil an economical source for biodiesel: A review. *Ind. Eng. Chem. Res.* **2006**, *45*, 2901–2913. [[CrossRef](#)]
11. Muniyappa, P.R.; Brammer, S.C.; Noureddini, H. Improved conversion of plant oils and animal fats into biodiesel and co-product. *Bioresour. Technol.* **1996**, *56*, 19–24. [[CrossRef](#)]
12. Dorado, M.P.; Ballesteros, E.; López, F.J.; Mittelbach, M. Optimization of Alkali-Catalyzed Transesterification of Brassica Carinata Oil for Biodiesel Production. *Energy Fuels* **2004**, *18*, 77–83. [[CrossRef](#)]
13. Antolín, G.; Tinaut, F.V.; Briceño, Y.; Castaño, V.; Pérez, C.; Ramírez, A.I. Optimisation of biodiesel production by sunflower oil transesterification. *Bioresour. Technol.* **2002**, *83*, 111–114. [[CrossRef](#)]
14. Patil, P.; Deng, S.; Isaac Rhodes, J.; Lammers, P.J. Conversion of waste cooking oil to biodiesel using ferric sulfate and supercritical methanol processes. *Fuel* **2010**, *89*, 360–364. [[CrossRef](#)]
15. Chhetri, A.B.; Watts, K.C.; Islam, M.R. Waste Cooking Oil as an Alternate Feedstock for Biodiesel Production. *Energies* **2008**, *1*, 3–18. [[CrossRef](#)]
16. Pinnarat, T.; Savage, P.E. Noncatalytic esterification of oleic acid in ethanol. *J. Supercrit. Fluids* **2010**, *53*, 53–59. [[CrossRef](#)]
17. Kusdiana, D.; Saka, S. Two-step preparation for catalyst-free biodiesel fuel production: Hydrolysis and methyl esterification. *Appl. Biochem. Biotechnol.* **2004**, *113–116*, 781–791. [[CrossRef](#)]
18. Bhargava, A.K.; Sharma, C.P. *Mechanical Behaviour and Testing of Materials*; PHI Learning Private Limited: Delhi, India, 2011.
19. Wan Omar, W.N.N.; Saidina Amin, N.A. Optimization of heterogeneous biodiesel production from waste cooking palm oil via response surface methodology. *Biomass Bioenergy* **2011**, *35*, 1329–1338. [[CrossRef](#)]
20. Lotero, E.; Liu, Y.; Lopez, D.E.; Suwannakarn, K.; Bruce, D.A.; Goodwin, J.G. Synthesis of biodiesel via acid catalysis. *Ind. Eng. Chem. Res.* **2005**, *44*, 5353–5363. [[CrossRef](#)]
21. Corma, A.; Garcia, H. Lewis acids: From conventional homogeneous to green homogeneous and heterogeneous catalysis. *Chem. Rev.* **2003**, *103*, 4307–4365. [[CrossRef](#)] [[PubMed](#)]
22. Okuhara, T. Water-tolerant solid acid catalysts. *Chem. Rev.* **2002**, *102*, 3641–3665. [[CrossRef](#)] [[PubMed](#)]
23. Yin, H.L.; Tan, Z.Y.; Liao, Y.T.; Feng, Y.J. Application of $\text{SO}_4^{2-}/\text{TiO}_2$ solid superacid in decontaminating radioactive pollutants. *J. Environ. Radioact.* **2006**, *87*, 227–235. [[CrossRef](#)] [[PubMed](#)]
24. Wang, J.; Yang, P.; Fan, M.; Yu, W.; Jing, X.; Zhang, M.; Duan, X. Preparation and characterization of novel magnetic $\text{ZrO}_2/\text{TiO}_2/\text{Fe}_3\text{O}_4$ solid superacid. *Mater. Lett.* **2007**, *61*, 2235–2238. [[CrossRef](#)]
25. Wen, Z.; Yu, X.; Tu, S.-T.; Yan, J.; Dahlquist, E. Biodiesel production from waste cooking oil catalyzed by $\text{TiO}_2\text{-MgO}$ mixed oxides. *Bioresour. Technol.* **2010**, *101*, 9570–9576. [[CrossRef](#)] [[PubMed](#)]

26. De Almeida, R.M.; Noda, L.K.; Gonçalves, N.S.; Meneghetti, S.M.P.; Meneghetti, M.R. Transesterification reaction of vegetable oils, using superacid sulfated TiO₂-base catalysts. *Appl. Catal. A Gen.* **2008**, *347*, 100–105. [[CrossRef](#)]
27. Li, Y.; Zhang, X.-D.; Sun, L.; Xu, M.; Zhou, W.-G.; Liang, X.-H. Solid superacid catalyzed fatty acid methyl esters production from acid oil. *Appl. Energy* **2010**, *87*, 2369–2373. [[CrossRef](#)]
28. Wang, J.-H.; Mou, C.-Y. Characterizations of aluminum-promoted sulfated zirconia on mesoporous MCM-41 silica: Butane isomerization. *Microporous Mesoporous Mater.* **2008**, *110*, 260–270. [[CrossRef](#)]
29. Wang, Y.; Gan, Y.; Whiting, R.; Lu, G. Synthesis of sulfated titania supported on mesoporous silica using direct impregnation and its application in esterification of acetic acid and n-butanol. *J. Solid State Chem.* **2009**, *182*, 2530–2534. [[CrossRef](#)]
30. Yadav, G.D.; Nair, J.J. Sulfated zirconia and its modified versions as promising catalysts for industrial processes. *Microporous Mesoporous Mater.* **1999**, *33*, 1–48. [[CrossRef](#)]
31. Minami, E.; Saka, S. Kinetics of hydrolysis and methyl esterification for biodiesel production in two-step supercritical methanol process. *Fuel* **2006**, *85*, 2479–2483. [[CrossRef](#)]
32. Hu, X.; Wei, T.; Liao, A.; Tong, Z. Use of acid cation-exchange resin for catalytic conversion of soybean acid oil to biodiesel. *J. Mater. Cycles Waste Manag.* **2016**, *18*, 123–131. [[CrossRef](#)]



© 2017 by the authors. Licensee MDPI, Basel, Switzerland. This article is an open access article distributed under the terms and conditions of the Creative Commons Attribution (CC BY) license (<http://creativecommons.org/licenses/by/4.0/>).